Biochimica et Biophysica Acta 1831 (2013) 327–340

Contents lists available at SciVerse ScienceDirect

Biochimica et Biophysica Acta

journal homepage: www.elsevier.com/locate/bbalip

Nuclear lipid droplets: A novel nuclear domain

J.P. Layerenza [a], P. González [b], M.M. García de Bravo [a], M.P. Polo [a], M.S. Sisti [a], A. Ves-Losada [a,c,*]

[a] INIBIOLP (CCT-La Plata-CONICET-UNLP), La Plata, Buenos Aires, Argentina
[b] Cátedra de Patología, Facultad de Ciencias Médicas, UNLP & CIC-Pcia, Buenos Aires, Argentina
[c] Departamento de Ciencias Biológicas, Facultad de Ciencias Exactas, UNLP, La Plata, Buenos Aires, Argentina

ARTICLE INFO

Article history:
Received 10 April 2012
Received in revised form 2 October 2012
Accepted 16 October 2012
Available online 23 October 2012

Keywords:
Nuclear neutral lipid
Nuclear domain
Lipid droplet
Endonuclear lipid
Triacylglycerol
Oleic acid

ABSTRACT

We investigated nuclear neutral-lipid (NL) composition and organization, as NL may represent an alternative source for providing fatty acids and cholesterol (C) to membranes, signaling paths, and transcription factors in the nucleus. We show here that nuclear NL were organized into nonpolar domains in the form of nuclear-lipid droplets (nLD). By fluorescent confocal microscopy, representative nLD were observed in situ within the nuclei of rat hepatocytes in vivo and HepG2 cells, maintained under standard conditions in culture, and within nuclei isolated from rat liver. nLD were resistant to Triton X-100 and became stained with Sudan Red, OsO4, and BODIPY493/503. nLD and control cytosolic-lipid droplets (cLD) were isolated from rat-liver nuclei and from homogenates, respectively, by sucrose-gradient sedimentation. Lipids were extracted, separated by thin-layer chromatography, and quantified. nLD were composed of 37% lipids and 63% proteins. The nLD lipid composition was as follows: 19% triacylglycerols (TAG), 39% cholesteryl esters, 27% C, and 15% polar lipids; whereas the cLD composition contained different proportions of these same lipid classes, in particular 91% TAG. The TAG fatty acids from both lipid droplets were enriched in oleic, linoleic, and palmitic acids. The TAG from the nLD corresponded to a small pool, whereas the TAG from the cLD constituted the main cellular pool (at about 100% yield from the total homogenate). In conclusion, nLD are a domain within the nucleus where NL are stored and organized and may be involved in nuclear lipid homeostasis.

1. Introduction

Cellular nuclei are an evolutionary development of the eukaryotic cell that enables a critical compartmentation of the processes of replication, transcription, pre-mRNA splicing, and ribosome assembly among other fundamental cellular functions.

Nuclear lipids play an active role in cell proliferation, differentiation, and apoptosis and are essential structural and functional components of the nucleus. The lipids, however, represent only 16% of the nuclear composition, with the remaining nuclear constituents consisting of proteins and nucleic acids [1,2].

In liver cells, the location of the nuclear lipids is not restricted to the nuclear membranes alone since the membrane-depleted nuclear matrix (Mx) constitutes a second lipid pool. The nuclear polar lipids (PL), particularly glycerophospholipids (GP)—though also found within the Mx—are, however mainly located in the nuclear membranes [3–5]. Moreover, Albi et al. determined that 10% of nuclear PL were associated with chromatin [4].

Up to now, since nuclear-lipid research has focused on PL, the information on neutral lipids (NL) is scarce. In 1970 Kleinig characterized triacylglycerols (TAG), cholesterol (C), and cholesteryl esters (CE) in the nuclei from pig liver [6], while Keenan et al. determined the composition of these same NL in nuclear membranes from bovine liver [7]. Later, TAG as well as CE and C were analyzed in nuclei from bovine and rat liver [8,9].

The aim of this work was to study nuclear-NL organization since those lipid species may represent alternative sources of nuclear fatty acids (FA) and signaling lipids to the nuclear membranes within locations for ready availability. Our hypothesis was that nuclear NL are organized within the nucleus in domains homologous to those of the cytosolic lipid droplets (cLD).

2. Materials and methods

2.1. Materials

Silica gel G precoated 20×20 cm thin layer chromatography (TLC) plates with or without a concentrating zone of 2.5×20 cm were from Merk (Buenos Aires, Argentina) and lipid standards from Nu-Chek Prep Inc. (Elysian, MN, USA). All chemicals and solvents were of analytical and HPLC grade, respectively. Rabbit polyclonal antibodies against ACAT-1 and Na^+/K^+−ATPase α, goat polyclonal antibodies against Lamin A, PLIN1 (perilipin) and SC-35; horseradish-peroxidase-conjugated (HRPc) rabbit anti(goat-IgG) antibody; and HRPc goat anti(mouse IgG) antibody

* Corresponding author at: INIBIOLP, Facultad de Ciencias Médicas, calles 60 y 120, 1900, La Plata, Argentina. Tel.: +54 221 482 4894; fax: +54 221 425 8988.
E-mail address: avlosada@biol.unlp.edu.ar (A. Ves-Losada).

1388-1981/$ – see front matter © 2012 Elsevier B.V. All rights reserved.
http://dx.doi.org/10.1016/j.bbalip.2012.10.005

were purchased from Santa Cruz, Biotechnology, Inc. (Santa Cruz, CA, USA). Rabbit antibody against the voltage-dependent–anion-channel protein (VDAC) was obtained from Thermo Scientific (Rockford, IL, USA), monoclonal antibodies against LAP2β and p54[nrb] from BD Biosciences (San Jose, CA, USA), HRPc goat anti(rabbit IgG) antibodies from Thermo Scientific (Rockford, IL, USA), Alexafluor-594-labeled chicken anti(mouse IgG) from Invitrogen (Buenos Aires, Argentina), and Cy3-labeled monkey anti(goat IgG) from Jackson ImmunoResearch (West Grove, PA, USA). The TAG Color Kit™ was from Wiener Laboratories (Rosario, Santa Fe, Argentina); DAPI, Sudan Red, and osmium tetroxide (OsO_4) from Sigma-Aldrich (St. Louis, MO, USA); and the BODIPY 493/503 from Invitrogen (Buenos Aires, Argentina).

2.2. Dye preparation

Solutions of BODIPY 493/503 stock (1 mg/ml), Sudan Red (0.5 mg/ml), and osmium tetroxide 2.5% [w/v] were prepared by dissolution in absolute ethanol, 70% [v/v] ethanol, and buffer A (1.4 mM/l NaH_2PO_4, 8 mM Na_2HPO_4, and 150 mM NaCl; pH 7.40); respectively.

2.3. Animals

Experiments were performed on 180 to 200 g 60 to 70 day-old male Wistar rats. The rats were housed in rooms with 12:12 h light–dark diurnal cycle (midnight being the midpoint of the dark period), and the experiments were performed in accordance with the Guide for Care and Use of Laboratory Animals (1996, National Academy Press). The animals were maintained on a commercial standard pellet diet (50% [w/w] Cargill mouse and rat chow, (Pilar, Buenos Aires, Argentina) and 50% [w/w] ACAI mouse and rat chow (San Nicolás, Buenos Aires, Argentina)) plus tap water *ad libitum*. The diet contained (by weight) 20% proteins and 4% total lipids with a FA composition of 15.6% 16:0, 1.1% 16:1, 6.3% 18:0, 26.9% 18:1 ($n-9$), 1.6% 18:1 ($n-7$), 42.7% 18:2 ($n-6$), 5.7% 18:3 ($n-3$), and trace amounts of 14:0, 20:4 ($n-6$), and 22:6 ($n-3$).

2.4. Preparation of rat-liver homogenates and nuclear fractions

Highly purified nuclei were isolated from liver homogenates by sucrose-gradient ultracentrifugation after the method of Blobel and Potter [10], as modified initially by Kasper [11], and then slightly further as follows: all rats were killed at 8 a.m. to equalize circadian-rhythm effects [12]. After decapitation, the animals were bled out freely and the excised livers first rinsed in cold buffer B (50 mM Tris–HCl, 2.5 mM KCl, 5 mM $MgCl_2$; pH 7.5) containing 0.25 M sucrose (buffer B-sucrose) and then immersed in ice before removal of connective tissue and weighing. The tissue was finely minced with scissors and washed two times with buffer B-sucrose. After addition of two volumes of this same solution per *g* liver and transfer to a 24-ml Potter–Elvehjem homogenizer equipped with a Teflon pestle, the tissue was homogenized at *ca.* 1,700 rpm. After about 15 up-and-down strokes to release the nuclei, the homogenate was filtered through four layers of cheesecloth. Of the collected filtrate, 8 ml were transferred to each of six 38.5-ml polyallomer tubes followed by 14 ml of 2.3 M sucrose in buffer B and the contents mixed by inversion. The homogenate was gradually underlayered with 3 ml of 2.3 M sucrose in buffer B. The nuclei were pelleted by centrifuging at 106,750 × *g* and 4 °C for 1 h. The heavy brownish-red plaque at the top of the tube was loosened by rimming with a small spatula and removed. The supernatant was decanted off by a quick inversion of the tube and then allowed to drain thoroughly. The residual sucrose solution was removed by squirting distilled water against the wall of the inverted tube without contacting the white nuclear pellet. After wiping the inside wall of the tube with an absorbent tissue, this wash was repeated followed by a final wash with buffer B. The nuclear pellet was then resuspended in 3 ml of 1.0 M sucrose in buffer B by agitation with a plastic stirring rod and the resuspension transferred to a 15-ml Dounce tissue grinder with a glass pestle. After homogenization and transfer to a 15-ml Corex centrifuge tube, the nuclei were sedimented at 4,100 × *g* and 4 °C for 10 min; the supernatant was discarded; and after resuspension in buffer B-sucrose, the nuclei were washed by a final centrifugation at 900 × *g* and 4 °C for 10 min.

In order to obtain the Mx, a quantitative removal of the nuclear envelope was effected by disruption of the nuclear-envelope with a low concentration (0.08%) of the nonionic detergent Triton X-100 followed by separation of the Mx on a sucrose gradient after the method of Vann et al. [13], slightly modified as follows [3]: after resuspension of the above pellet in 0.25 M sucrose in buffer C (10 mM Tris–HCl, 2 mM $MgCl_2$; pH 7.5) to give a final concentration of 8 mg protein/ml, a 0.5-ml aliquot was mixed with 20 ml of ice-cold 0.29 M sucrose in buffer D (5 mM Tris–HCl, 5 mM $MgCl_2$, 1.5 mM KCl, 1 mM EGTA; pH 7.4; containing 0.08% [v/v] Triton X-100) and incubated on ice for 20 min. The Mx were sedimented at 165 × *g* and 4 °C for 6 min, the supernatant removed, and the pellet resuspended

5 min with buffer I and incubated for 1 h at room temperature under gentle shaking with the following secondary-HRPc-antibody dilutions in buffer I containing 1% (v/v) nonfat milk: anti(rabbit IgG) 1:5,000, anti(goat IgG) 1:3,000, and anti(mouse IgG) 1:5,000. Membranes were washed 6 times with buffer I, 5 min each. The peroxidase activity was revealed by means of the Pierce ECL Western-blotting substrate (Pierce, Rockford, IL, USA) before chemiluminescence image acquisition with an ImageQuant 350 (GE Health Care, Buenos Aires, Argentina).

2.7. Lipid analysis

Lipids, extracted by the procedure of Folch et al. [21], were recovered from the chloroform layer and separated into different classes by TLC on plates precoated with silica gel G without concentrating zones. Samples were resolved up to half of each plate, with 80:20:1 (v/v/v) hexane/diethylether/acetic acid being used as mobile phase to separate the NL [22]. After visualization of the lipid species by exposure to iodine vapor, PL, diacylglycerides (DAG), C, free FA, TAG, and CE were located by comparison to the corresponding positions of known standards with respective retention factors of 0.06, 0.13, 0.18, 0.27, 0.60, and 0.96.

The PL (GP + sphingolipids [SP]) were scraped off the plate for quantification by the spectrometric determination of phosphorus [23]. To separate and quantify the C and CE, the sample was developed on TLC plates along with different concentrations of pure standards, the lipid spots revealed after spraying with acidic ferric-chloride solution, and the staining densities quantitated through the use of ImageJ software (National Institutes of Health, Bethesda, MD, USA) [24].

The TAG scraped off the plates were quantified by means of a kit assay procedure based on the liberation of glycerol through lipase-catalyzed hydrolysis (TAG Color, Wiener Lab., Rosario, Santa Fe, Argentina).

2.8. Analysis of fatty acid composition of total triacylglycerols

The TAG scraped off the TLC plates were extracted with chloroform and FA methyl esters prepared according to the method of Morrison and Smith [25] and analyzed by gas–liquid chromatography in a Hewlett-Packard HP 6890 apparatus (Wilmington, DE, USA). Samples were injected into a 30-m Omega Wax 250 (Supelco, Bellefonte, PA, USA) capillary column of i.d. 0.25 mm and a 0.25 μm film and the temperature programmed to obtain a linear increase of 3 °C/min from 175 to 230 °C. Chromatographic peaks were identified by comparison of their retention times with those of authentic standards.

2.9. Liver squash

After fixation of a slice of liver tissue by overnight incubation with 4% (v/v) formaldehyde in buffer B at 4 °C, a small piece was deposited onto a microscope slide, washed with 0.25 M sucrose in buffer B, and stained at 4 °C. The squash was done by applying minimal pressure from above with a coverslip, and the excess liquid was then removed.

2.10. Cell culture

HepG2 cells from American Type Culture Collection (ATCC HB-8065) were maintained and grown at 37 °C in surface culture attached to 95-cm^2 flasks, in Eagle's minimal essential medium containing 2 mM L-glutamine, 2.2 g/l sodium bicarbonate, 0.1 mM nonessential amino acids, 1.0 mM sodium pyruvate, and 10% (v/v) heat-inactivated fetal-bovine serum (Gibco, Grand Island, NY, USA) plus 0.1 g/l streptomycin. The cells were plated on coverlips and cultivated as previously described [26].

2.11. Bright-field microscopy

Ten microliters of sample suspensions were transferred to coverslips and kept on ice. Three alternative fixation methods were used: (1) air drying for 10 min, (2) incubation with OsO_4 solution for 10 min in the dark, or (3) incubation in 4% (v/v) formaldehyde in buffer A for 10 min at room temperature. Samples from the isolated bands were always fixed by method (1). Two alternative methods of staining were used. Samples were covered with Sudan-Red solution and incubated for 10 min, or with osmium-tetroxide solution and incubated on ice in the dark for 10 min, before analysis. Samples were examined by bright-field microscopy under an Olympus BX51 epifluorescence microscope (Shinjuku, Tokyo, Japan) through the use of the Image-Pro plus version 5.1 software (Media Cybernetics Inc, Bethesda, MD, USA).

2.12. Confocal laser-scanning microscopy

Coverslips with nuclei, Mx, HepG2 cells, or rat-liver squash were kept on ice and fixed by overnight incubation with 4% (w/v) paraformaldehyde in buffer J–sucrose (1.5 M KCl, 1.6 mM N-acetylcysteine, 4.7 mM potassium phosphate, 0.25 M sucrose; pH 7.4). Samples were washed 3 times with buffer J-sucrose after incubating sequentially for 10, 10, and 5 min per wash. Permeabilization was effected by incubation with 0.08% (v/v) Triton X-100 in buffer J-sucrose for 20 min. Samples were washed 4 times with buffer J-sucrose after incubating sequentially for 10, 10, 10, and 5 min per wash. For immunofluorescence, samples were incubated for 48 h with the respective primary-antibody dilutions (1:25 for anti-SC-35, 1:250 for anti-p54 [nrb], 1:100 for anti-LAP2β) in 1% (w/v) bovine-serum albumin in buffer J. After three washes of 10 min each, samples were incubated with DAPI (final concentration, 1 μg/ml) or BODIPY 493/503 (final concentration, 1 μg/ml) and the respective secondary-antibody dilutions (1:250 for both chicken anti[mouse IgG] alexa594 and monkey anti [goat IgG] Cy3) for 1 h. After three 10-min washes with buffer J-sucrose, the samples were mounted and observed. Images of fixed nuclear samples were examined with an Olympus (Shinjuku, Tokyo, Japan) confocal laser-scanning microscope (Fluoview FV1000, software version 1.7.3.0) mounted on an Olympus BX61 upright frame microscope, equipped with a 405-nm, a 473-nm, and a 559-nm diode laser and containing a UPLSAPO 40× (0.95 NA) objective. Ten representative fields containing several nuclei were selected. For nuclear-domains, Z-planes of 0.20- or 0.68-μm thickness were acquired. Z-plane cross-sections across the central position of a nucleus were obtained and the different planes reconstructed.

2.13. Image analysis

For determination of the diameters of nuclei, Mx, nLD, and cLD we used Image-Pro plus version 5.1 software (Media Cybernetics Inc., Bethesda, MD, USA) and for 3D reconstructions ImageJ (National Institutes of Health, Bethesda, MD, USA) and Amira ResolveRT 4.0 (Visaje Imaging Inc., San Diego, CA, USA) software.

2.14. nLD isolation

In order to isolate nLD, we adapted the standard procedure for cLD isolation by separation on a sucrose gradient after the method of Ontko et al. [27]. Thus, for nLD, isolated nuclei from 8 to 10 livers (200 mg of nuclear proteins) were pooled and resuspended in buffer B containing 1 M sucrose at a final volume of 2.5 ml. PMSF at a final concentration of 1 mM was added to inhibit proteolysis, and the pooled nuclei were kept on ice and sonicated in a Branson 450 Sonifier (Danbury, CT, USA) at a duty cycle of 50% and a setting 6.0, for 10 pulses 10 times followed by 20 pulses 5 times. Sonicated nuclei were then mixed with buffer B containing 2.3 M sucrose to give a

final sucrose concentration of 1.9 M in a final volume of 7.5 ml. As a control of the nLD-isolation method, liver cLD were isolated under the same conditions. Liver homogenate, obtained in buffer B-sucrose (*cf.* Section 2.4), was mixed with buffer B containing 2.3 M sucrose to give—as with the nLD—a final concentration of 1.9 M sucrose in 7.5 ml. A discontinuous sucrose gradient was prepared as follows: 1.5 ml of double-distilled water was added to a thick-walled polycarbonate ultracentrifuge tube. Then 2.5 ml of 0.3 M sucrose, 2.5 ml of 0.7 M sucrose, 3 ml of 1.0 M sucrose, 3 ml of 1.3 M sucrose, and

3. Results

3.1. Integrity and purity of nuclei

In isolated nuclei endoplasmic reticulum could be a troublesome contaminant since the outer nuclear membrane is a continuation of that cytoplasmic organelle. Those membranes are furthermore the most diffi

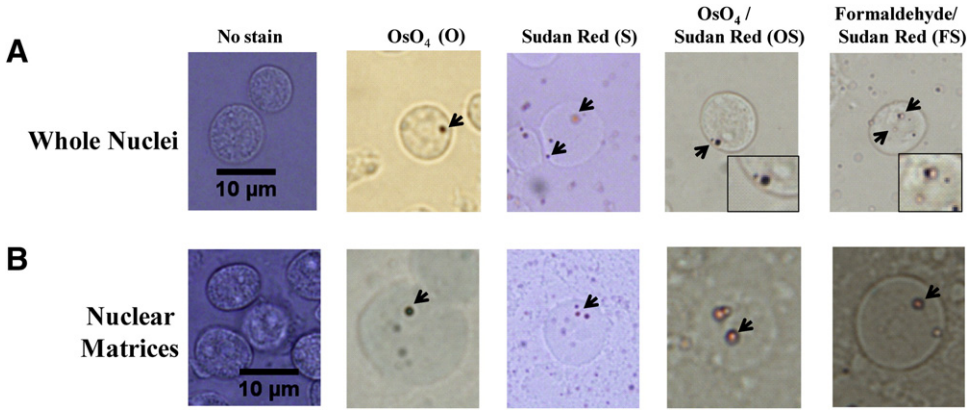

Fig. 2. Analysis of nuclear-lipid droplets from rat liver by microscopy. (A) Isolated whole nuclei and (B) Nuclear matrix (membrane-depleted nuclei) were stained and examined by bright-field microscopy. Sudan Red (S) and osmium tetroxide (O, OsO_4) were used as dyes. Staining was carried out over fixed (by formaldehyde (F) or O) and unfixed samples. Arrows point to the nLD. Inserts show detailed regions. The photographs correspond to representative observations.

having different sizes and characterized by a high proportion that were smaller than the median value.

In order to obtain further information about the localization and distribution of the nLD, we performed confocal microscopy (Fig. 3). As observed in the orthogonal views and 3D reconstructions, nLD were localized within the nuclei and were furthermore confined to the Mx domains (Fig. 3A and Video 1).

We also first labeled the liver nuclei and the Mx with DAPI and LAP2β (the latter binding to nuclear lamina) and subsequently stained the nLD with BODIPY 493/503 (Fig. 3B and C). Merge images revealed the nLD to be localized within the nucleus beneath the LAP2β and thus interacting with the nuclear lamina. The two analyses indicated that nLD were both endonuclear and confined to the Mx domain: this localization in the Mx once again pointed to their resistance to Triton X-100.

In order to analyze the spatial relationship between nLD and other domains within the nucleus, nuclei were stained with speckles- and paraspeckles-marker proteins (SC-35 and p54[nrb], respectively) and visualized by immunofluorescence microscopy (Fig. 4). As expected from the literature [35,36], many speckles and paraspeckles were observed by immunofluorescence within the nucleus, but those domains were not colocalized with the nLD (Fig. 4). The random distribution of nLD previously observed in Figs. 2 and 3 was corroborated here since nLD were recorded both in a central localization (Fig. 4A) and close to the nuclear membrane (Fig. 4B).

To further corroborate our findings, nLD were visualized both in hepatocytes from the livers of rats maintained on a standard diet (Fig. 5) and in HepG2 cells cultured under standard conditions (Fig. 6). Cells from each source were labeled with DAPI and the nLD as well as the cLD subsequently stained with BODIPY 493/503. In both preparations cLD were observed as well by confocal microscopy (Figs. 5 and 6). Merge images showed the nLD to be localized within the nucleus and randomly distributed (Figs. 5 and 6).

Both of these cell types were also stained with Sudan Red and OsO_4 (data not shown), where the LD, though clearly visible, failed to stand out in bold relief because of the stained background; but in spite of that background staining within the cell, the diameter measurements were nevertheless found to be comparable to those indicated by BODIPY staining (fluorescence microscopy), where no background is present (Supplementary Table 2). As stated above with respect to LD in isolated nuclei and Mx, the true size of nLD and cLD observed in the hepatocytes *in vivo* or the HepG2 cells in culture (Figs. 5 and 6) could not be determined since both types of LD could only be visualized after staining (Supplementary Table 2). Nonetheless, we can consider that the diameter of nLD was between 0.57 and 0.90 µm (median) and was comparable to that estimated for nLD in isolated nuclei (Fig. 2 and Supplementary Table 1). In both of these cell types, cLD were a larger-sized population than nLD with maximum diameters at between 2.39 and 3.67 µm as opposed to 0.84 – 1.49 µm. As expected, nLD and cLD had the same apparent minimum diameter since the smallest LD that can be observed is limited by the resolution of the microscope. For this reason, however, the true minimum diameter of each type of lipid droplet cannot be determined with certainty given the technology available. As observed for nLD from isolated nuclei (Fig. 2, Supplementary Table 1), the results of quartile analysis of nLD and cLD diameters from these whole cells in all stained samples indicated that both of these LD were characterized by a heterogeneous droplet population with different sizes and a high proportion of LD smaller than mean value (Supplementary Table 2).

In conclusion, nLD could be visualized within the nucleus as discrete spheres with a random distribution and representing an extremely small nuclear domain. nLD were smaller than cLD, were fewer in number, and could be observed not only within isolated rat-liver nuclei and Mx but also within the nuclei from intact rat-liver hepatocytes and whole HepG2 cells.

3.4. Isolation of nLD from isolated rat-liver nuclei

nLD were isolated from a sample of intact nuclei by an adaptation of a standard procedure for cLD isolation based on separation by means of a sucrose-density gradient [27]. As a control for the method, cLD were isolated in parallel from a liver homogenate. Whereas 6 bands became equilibrated in layers within the gradient from the liver homogenate, only one band (α) was resolved at the top of the tube when the sample from whole nuclei was centrifuged in the density gradient (Fig. 7).

Although this single band (α) was detected in the sucrose gradient from the nuclear sample (nLD), we cannot discard the possibility that within the nucleus, LD populations of different compositions are also present as in the cytosol; but because of the low concentration of NL components, they were impossible to be visualized as bands or quantify by this procedure.

When the nuclear α band and the cytosolic A band were qualitatively analyzed by transmission electron microscopy, in both samples clusters of spherical droplets with diameters ranging from 30 to 80 nm were visualized (Fig. 8A). Moreover, in both α and A bands, we observed Sudan-Red-positive spherical LD of different sizes with diameters ranging from 0.5 to 27 µm (Fig. 8B). In this regard, the observation of α and A bands should be done immediately after staining since isolated LD usually cluster into fewer and larger-sized droplets (not shown). This clustering would explain the differences observed

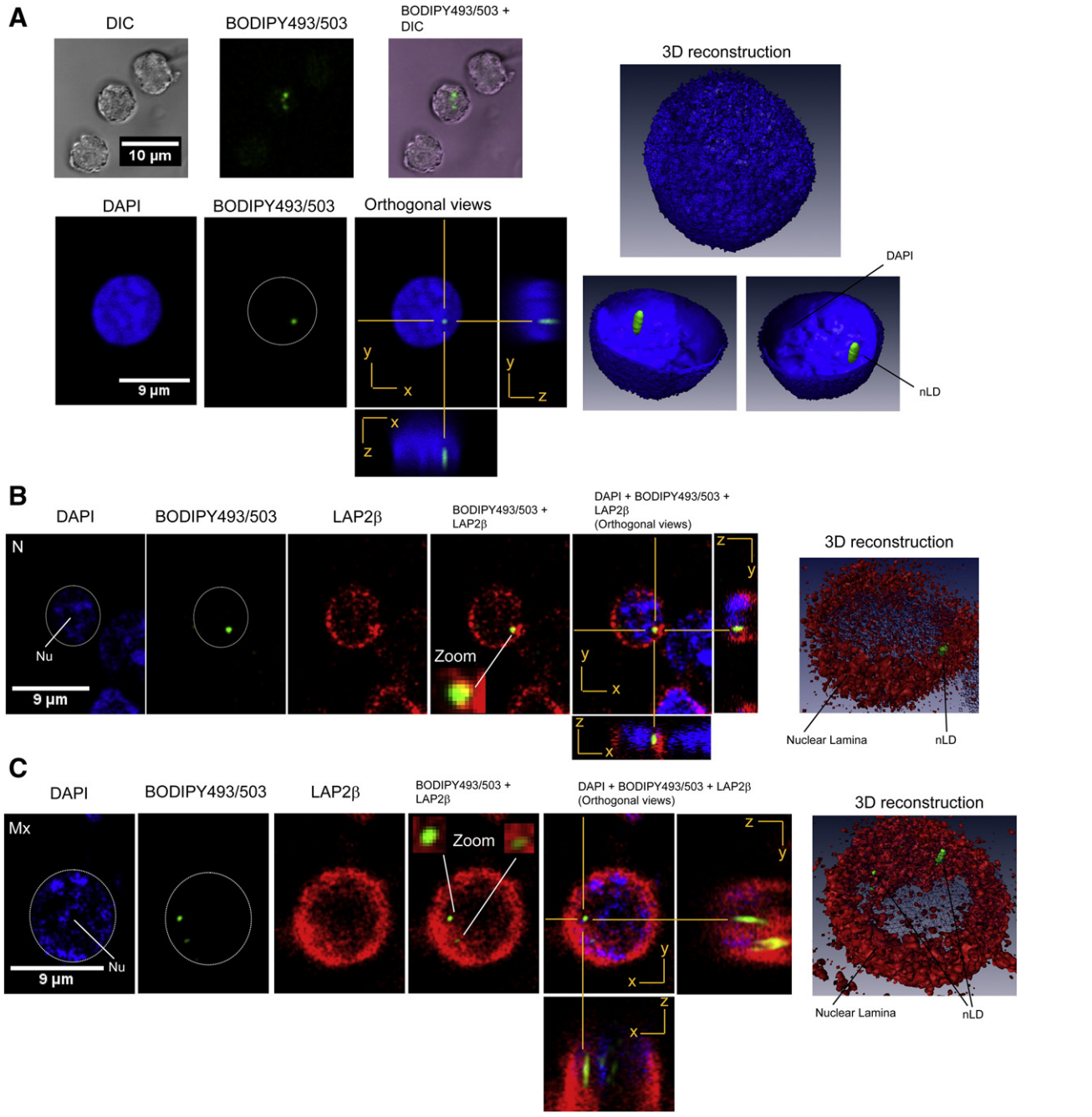

Fig. 3. Analysis of isolated nuclei from rat liver by confocal laser-scanning microscopy. (A) Nuclei (N) and nuclear-lipid droplets (nLD) were stained with DAPI (blue) and BODIPY 493/503 (green), respectively, and observed by confocal laser-scanning microscopy. Nuclei were also observed with the transmitted-light channel of the confocal microscopy (DIC, differential interference contrast). The nLD localization in (B) nuclei and (C) the nuclear matrix (Mx) was analyzed by immunofluorescence. The nuclear lamina was stained with antibodies against LAP2β (in red). Z-plane cross-sections through the central position of a nucleus were obtained and the different planes reconstructed to give XZ and YZ orthogonal projections. Three-dimensional reconstructions were performed and the nLD and nuclear lamina visualized through isosurface rendering (green and red, respectively) and through outline rendering by DAPI (blue). The photographs correspond to representative observations. Nu, nucleolus.

between LD diameters present in the bands from isolated nuclei or the homogenates and the original intact structures (i.e., nuclei, Mx, hepatocytes, and HepG2 cells) since after fixation no such clustering had been present (*cf.* Figs. 2–6). Moreover, methyl and ethyl alcohols routinely used in fixation and staining have been seen to modify both the number and size of cLD [34,37].

Based on these results and the above considerations, we conclude that nuclear α band consisted in spherical droplets (i.e., nLD) that can be stained by Sudan Red in the same manner as cLD.

3.5. nLD lipid composition

For the determination of the lipid classes, isolated α band containing nLD was extracted and lipids separated by TLC along with standards (Fig. 9). These lipids were composed of TAG, C, and CE along with low amounts of free FA and PL (GP + SP). In a similar fashion, cLD lipids were extracted from the sucrose-density-gradient A band (Fig. 7). Table 2 shows the NL composition along with PL and protein content of nLD and cLD.

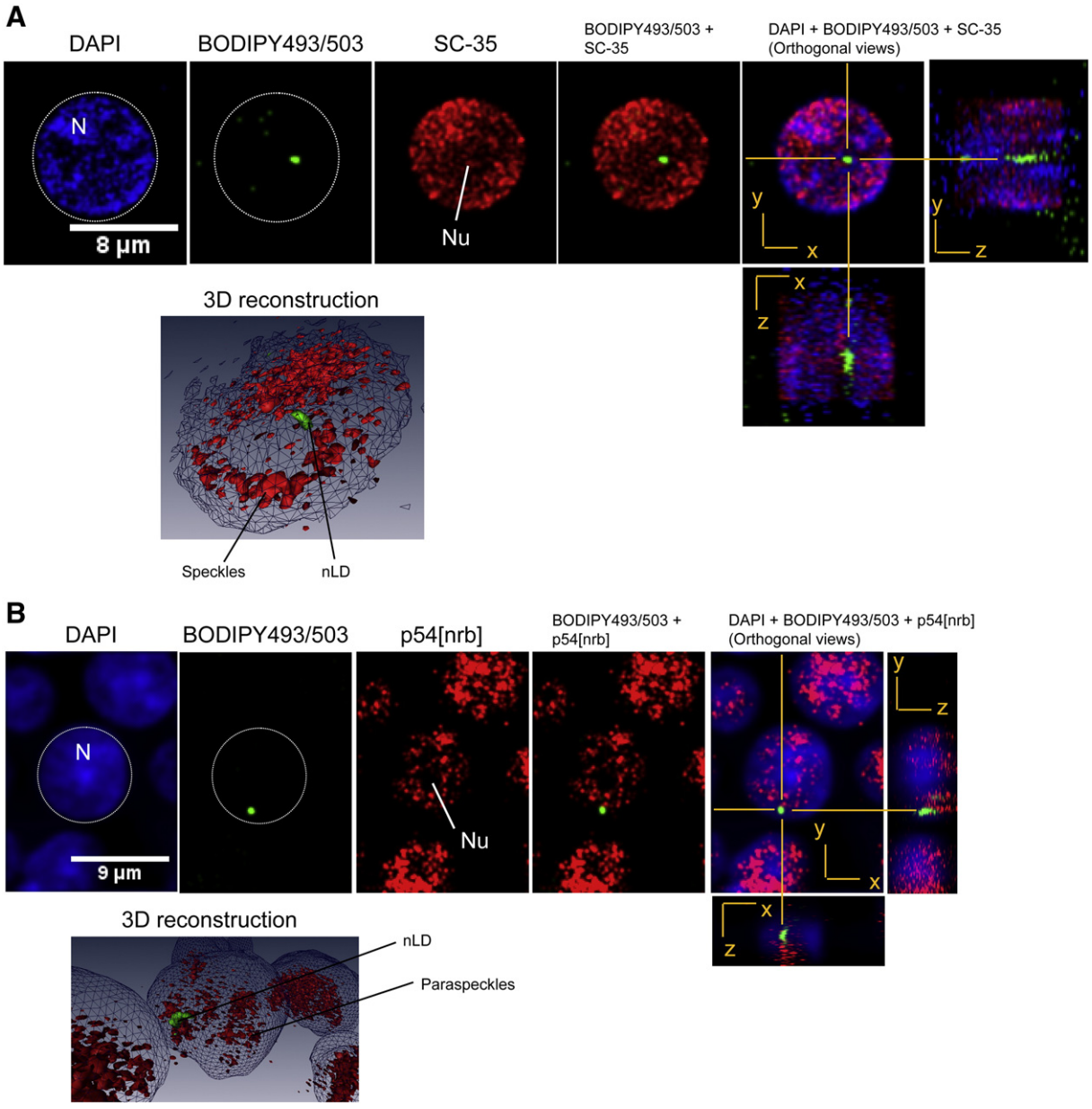

Fig. 4. Spatial relationship of nuclear-lipid droplets to known nuclear domains. Spatial relationship of nuclear-lipid droplets (nLD) to nuclear domains was analyzed by immunofluorescence and observed by confocal laser-scanning microscopy. The (A) speckles and (B) paraspeckles were stained with antibodies against SC-35 and p54[nrb], respectively (shown in red). Z-plane cross-sections through the central position of a nucleus were obtained and the different planes reconstructed to give XZ and YZ orthogonal projections. Three-dimensional reconstructions were performed and the nLD and nuclear domains visualized through isosurface rendering by the antibodies (green and red, respectively) and outline rendering by DAPI (blue). Photographs correspond to representative observations. N, Nucleus; Nu, nucleolus.

nLD were composed of 38% lipids and 62% proteins by weight (µg/g liver). nLD lipids and proteins represented an exceedingly small proportion of the total cell components, as the yields of these species from the homogenate were lower than 0.002%. nLD lipids consisted in mainly NL (85%) along with a small proportion (15%) of PL (Fig. 10).

nLD total PL were quantified by the phosphorus content of the corresponding TLC spot but were not further separated into different GP or SP classes because of the low amounts of these components in the samples. These nLD PL are probably composed of GP as well as SP, since those lipid classes had been found to be the PL components of the Mx [3].

nLD from liver exhibited an NL composition rich in TAG (23%), CE (45%), and C (32%) (Table 2). Fig. 10 illustrates that nLD-lipid composition was markedly different from that observed in liver homogenates, whole nuclei, Mx, and cLD A band. Table 2 shows cLD lipid composition and protein content. Of the six sucrose-gradient bands isolated from total liver homogenate, only the A band was analyzed since this band had an equivalent position and thus a comparable density to that of α band isolated on the sucrose gradient of the nuclear sample (Fig. 7). As expected, the cLD A band had a total-lipid composition equivalent to that reported previously [27].

These cLD—consisting of 78% lipids and 22% proteins by weight (µg/g liver)—had a very different overall composition from that of the nLD (Table 2) and furthermore contained almost exclusively NL (99.4%) along with an extremely low proportion (0.6%) of PL (Fig. 10). The NL of the cLD, in turn, consisted principally in TAG (88%) with low amounts of CE (5%) and C (7%). The composition of the 6 bands of cLD isolated from rat liver by Onko et al. were all different from that of the present nLD α band [27]. This observation is highly relevant to the issue of the uniqueness of the nLD.

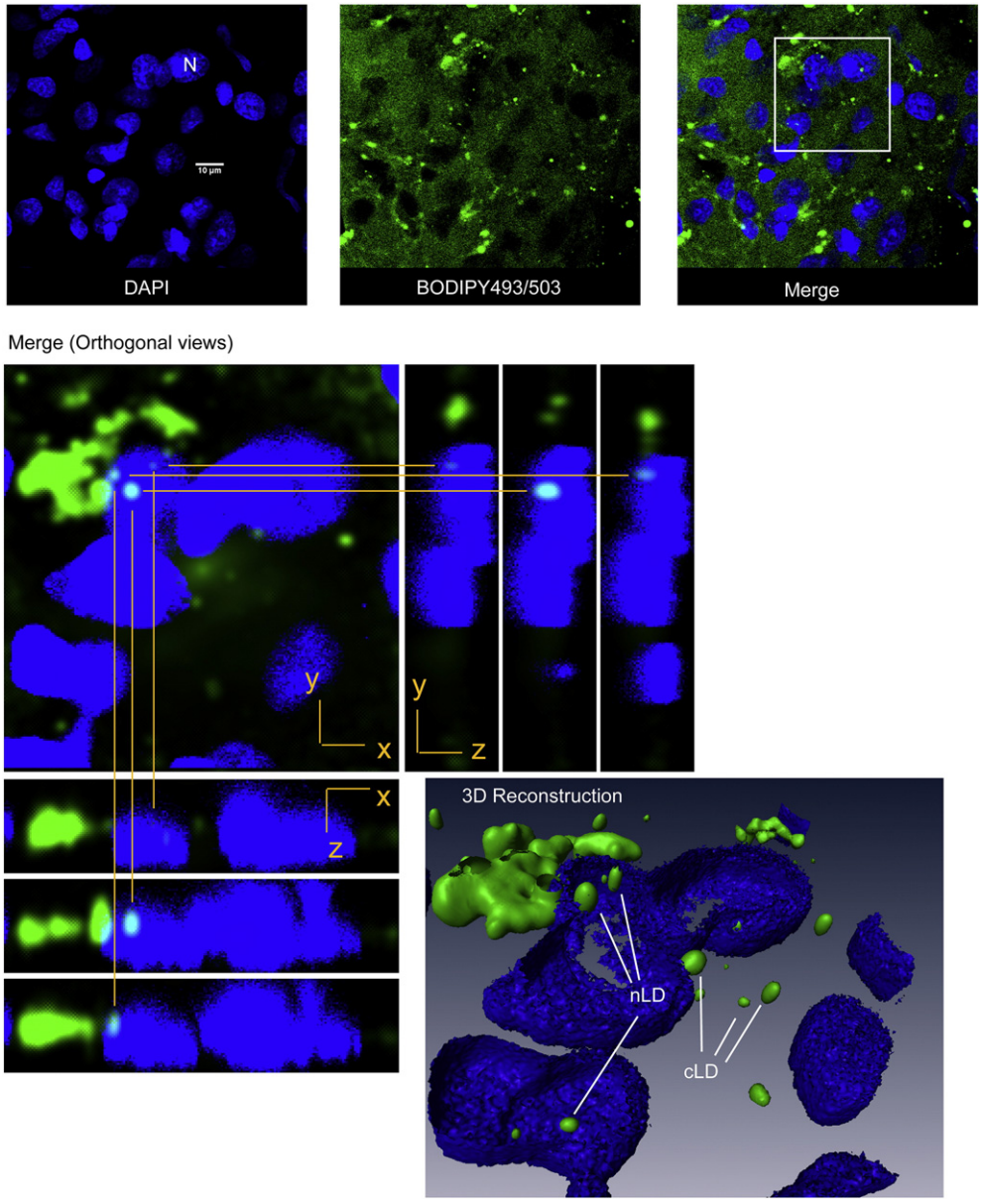

Fig. 5. Microscopical analysis of nuclear- and cytosolic-lipid droplets from rat hepatocytes. Rat-liver squashes were stained and analyzed by confocal laser-scanning microscopy. Staining was carried out on fixed samples. Nuclei (N) and nuclear- and cytosolic-lipid droplets (nLD and cLD) were stained with DAPI (blue) and BODIPY 493/503 (green), respectively. Z-plane cross-sections through the central position of a nucleus were obtained and the different planes reconstructed to give XZ and YZ orthogonal projections. Three-dimensional reconstructions were performed and the LD visualized through isosurface rendering by BODIPY (green) and outline rendering by DAPI (blue). Photographs correspond to representative observations.

The cytosolic TAG from cLD constituted the main hepatocyte TAG pool since the yield from homogenate was about 100%. In contrast, nLD TAG consisted in a quantitatively small overall cellular pool along with the different subcellular localization. Supplementary Table 3 shows the composition of TAG FA from rat-liver nLD and cLD. FA composition of TAG from nLD was in agreement with previous results from an analysis of the TAG from whole nuclei [38]. In both of those LD fractions, the TAG FA were composed of equivalent proportions of saturated (30%), monounsaturated (MUFA), and polyunsaturated FA (PUFA). MUFA and PUFA from the series $n-9$ (30–32%) and $n-6$ (28–30%) were the most prevalent unsaturated fatty acids present. Finally, within nLD the main fatty acids esterified to TAG were oleate (18:1 $n-9$) and linoleate (18:2 $n-6$) plus to a lesser extent palmitate (16:0).

In conclusion, our findings have indicated that the nLD are a supramolecular nuclear structure mainly composed of TAG, C, and CE along with a low percentage of PL and proteins.

4. Discussion

We have demonstrated that nuclear NL are organized in discrete nonpolar domains within the nucleus analogous to the cytosolic lipid droplets, the nuclear-lipid droplets (nLD). This nuclear domain was furthermore found to be constituted by a few number of small droplets randomly distributed within the nucleus with a spatial localization that differed from those of the lamina, speckles, paraspeckles, and nucleolus—as visualized by immunofluorescence microscopy. nLD were moreover resistant to the nonionic detergent Triton X-100.

nLD were observed in isolated nuclei from rat liver as well as in rat-liver hepatocytes and HepG2 cells maintained under standard nutritional conditions (with respect to diet or culture medium, respectively) and normal (not pathological) states. nLD from both rat hepatocytes and HepG2 cells were smaller in size than the cLD, in agreement with the nLD–composition data. If we consider that nLD

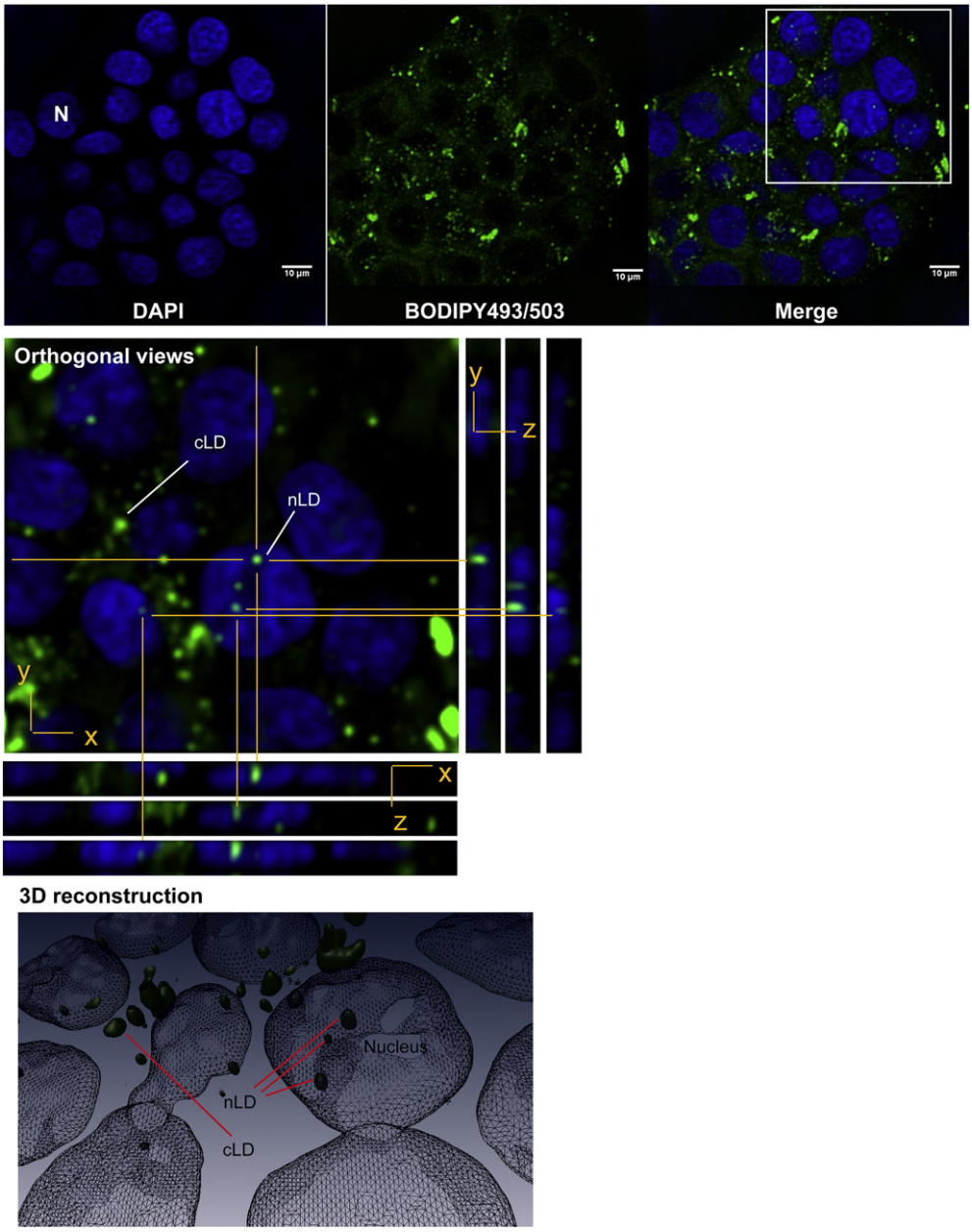

Fig. 6. Microscopical analysis of nuclear- and cytosolic-lipid droplets from HepG2 cells. HepG2 cultured cells were stained and analyzed by confocal laser-scanning microscopy. Staining was carried out on fixed samples. Nuclei (N) and nuclear- and cytosolic-lipid droplets (nLD and cLD) were stained with DAPI (blue) and BODIPY 493/503 (green), respectively. Z-plane cross-sections through the central position of a nucleus were obtained and the different planes reconstructed to give XZ and YZ orthogonal projections. Three-dimensional reconstructions were performed and the LD visualized through isosurface rendering by BODIPY (green) and outline rendering by DAPI (blue). Photographs correspond to representative observations.

were organized around a hydrophobic core of TAG and CE surrounded by a monolayer of PL, C, along with the associated proteins—as in cLD [33]—then, from data of Table 2 (expressed as μg/g liver), we can calculate the proportion of the monolayer and of the hydrophobic-core components that are present in each of the two LD types. The nLD monolayer constituents (proteins, PL, and C) would represent 80% of the total LD components, whereas these species constitute only 24% in cLD. Therefore, a greater proportion of the surrounding monolayer in nLD would indicate that within the nucleus the nLD should be smaller than cLD since a greater fraction of monolayer would be necessary to cover a much smaller volume of each hydrophobic core. Interestingly, nLD are apparently surrounded by a monolayer organization similar to that of cLD—it composed of 80–90% proteins and 10–20% lipids, the latter being 20–30% PL and 70–80% C. Smaller LD than the cLD have also been reported within other organelles, such as the endoplasmic reticulum and the Golgi apparatus [39].

All nuclear TAG were found to be localized in the Mx, and organized in the form of nLD. Since the molar ratio of PL to TAG in nLD was 0.75 (expressed as nmol per g liver) and the Mx TAG content was 1.7 nmol per g liver, then about 1.3 nmol of PL per g liver would constitute the monolayer required to surround that total amount of TAG within nLD. Since the total PL content of the Mx was 4.3 nmol per g liver, approximately one third of Mx PL were located in nLD monolayer with the remaining two thirds of the PL being associated with another endonuclear-lipid domain. Furthermore, the PL clearly represent a greater proportion of the lipids in the Mx (at 58%) than in the nLD (at only 15%). Nuclear speckles constitute a possible endonuclear domain where the remaining two-thirds of Mx PL

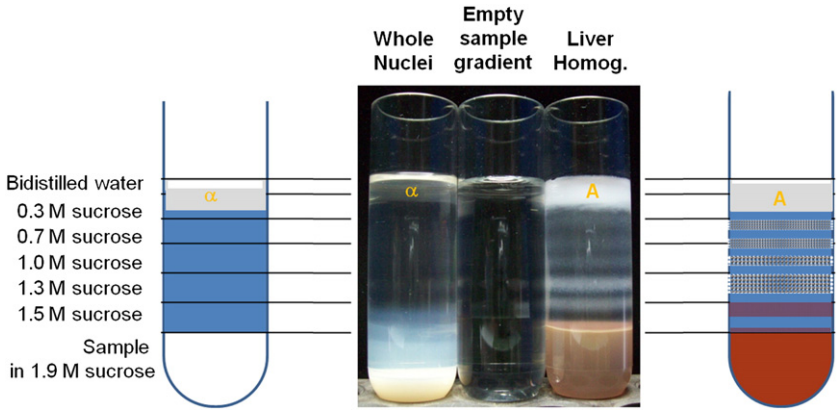

Fig. 7. Isolation of nuclear-lipid droplets from rat liver. Photograph of tubes following 30 min of discontinuous sucrose-gradient centrifugation of whole nuclei, the empty-gradient control, and liver homogenate. Bands were photographed with ordinary top lighting and a black background. Under these conditions, 6 bands that equilibrated in layers within the gradient are visible in the liver homogenate (the uppermost being the A band) and only one band (α) at the top of the tube in the sample of whole nuclei. The sample residue and a pellet remain at the bottom of the tube (with the homogenate or whole nuclei). Schematics of the tubes along with the flotation locations of the bands are also represented on both sides.

could be located since these speckles have been recently found to be involved in the synthesis nuclear phosphatidylcholine (PC). Moreover, the enzymatic activity of the nuclear CTP-phosphocholine cytidylyltransferase is regulated by a translocation of the enzyme between speckles and the nuclear membrane [40].

Within the nucleus, PL were also found to be associated with chromatin [41]; with the principal subclasses being PC, phosphatidylethanolamine (PE), phosphatidylinositol (PI), phosphatidylserine (PS) and sphingomyelins (SM).

The nLD PL classes could not be determined because of the small amount of PL; but as quantified in the Mx, PC and PE were the most abundant classes, followed by equivalent proportions of PI, PS, SM, and lysoPC [3]. GP along with the SP of the Mx might well be components of nLD monolayer [3]. Barts et al. [42] characterized the PL composition of cLD isolated from different cell lines and determined that PC was the most abundant PL class followed by PE, PI, and ether-linked PC, lysoPC, lysoPE, with only very low levels of SM and PS being present.

C has also been described as associated with chromatin in the nucleus [41]—there both in a soluble pool and linked to a complex formed by SM and proteins. On the basis of our results, we believe that at least part of the nLD-monolayer components were those of the complex already described by Cascianelli et al. for rat-liver nuclei and composed of C, SM, and proteins [43]. In this regard, the C in the

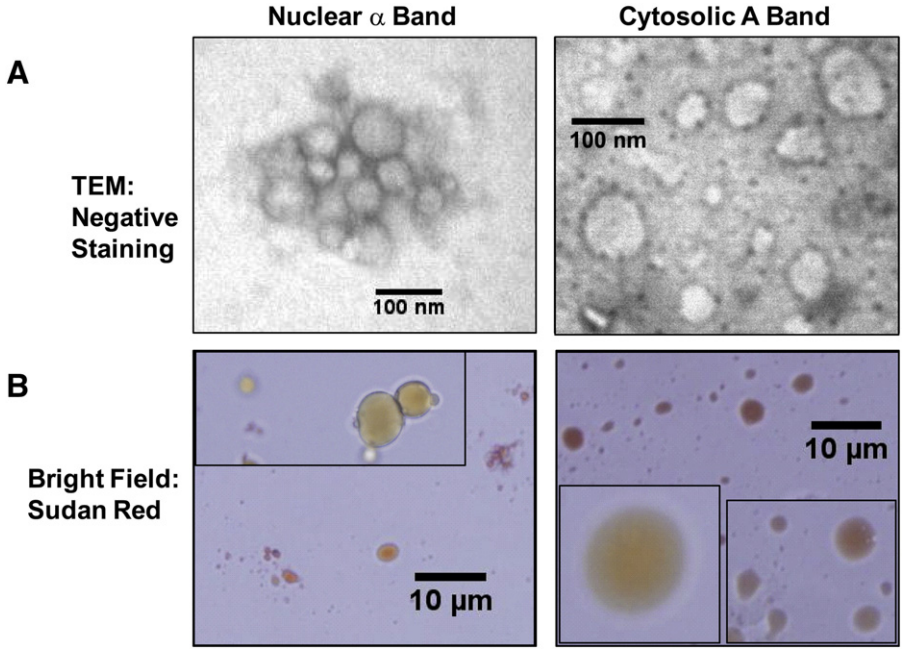

Fig. 8. Analysis of isolated nuclear-lipid droplets from rat liver by microscopy. Lipid droplets (LD) isolated from nuclei (α band) and from liver homogenate (A band) by sucrose-density gradients as indicated in Fig. 7 were analyzed by (A) transmission electron microscopy after negative staining with sodium phosphotungstate (scale bar, 100 nm) and (B) bright-field microscopy after Sudan-Red staining (scale bar, 10 μm). The photographs were taken from representative observations. Inserts correspond to LD from several fields obtained at the same magnification showing the wide degree of size heterogeneity present in a representative preparation. (For interpretation of the references to color in this figure legend, the reader is referred to the web version of this article.)

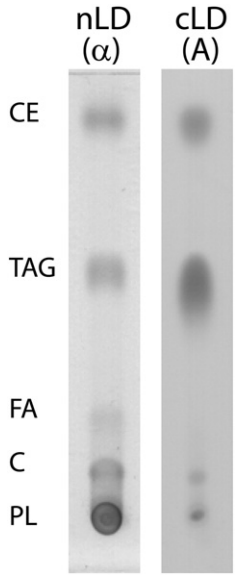

Fig. 9. Composition of nuclear-lipid droplets from rat liver. Lipids from α (nLD) and A (cLD) sucrose-gradient bands were extracted and separated into different classes by thin-layer chromatography with hexane/diethylether/acetic acid [80:20:1, v:v:v] as the mobile phase and visualized after $FeCl_3$-H_2SO_4-acetic acid charring. PL, polar lipids; C, cholesterol; FA, free fatty acids; TAG, triacylglycerols; and CE, cholesteryl esters.

monolayer of nLD would presumably be in the nonesterified form and, as such, involved in nuclear-lipid metabolism; whereas the CE in the nLD hydrophobic core would function as a storage molecule. Proteins involved in C and SM metabolism as well as those in the SM-signaling processes could likewise be associated with the nLD monolayer. At all events, the cLD monolayer has been reported to have very low proportions of SM and PS [42].

Exogenous FA, either free or bound to L-FABP, have been previously reported to be esterified into nuclear and Mx PL and NL (TAG and DAG) [38] by an acyl-CoA-dependent mechanism [44–46]. Since the present findings indicate the Mx TAG to be located exclusively in the nLD, we now know that in those previous experiments the nLD TAG were being labeled. On the basis of these observations, nLD can thus be regarded as a domain with an active lipid metabolism.

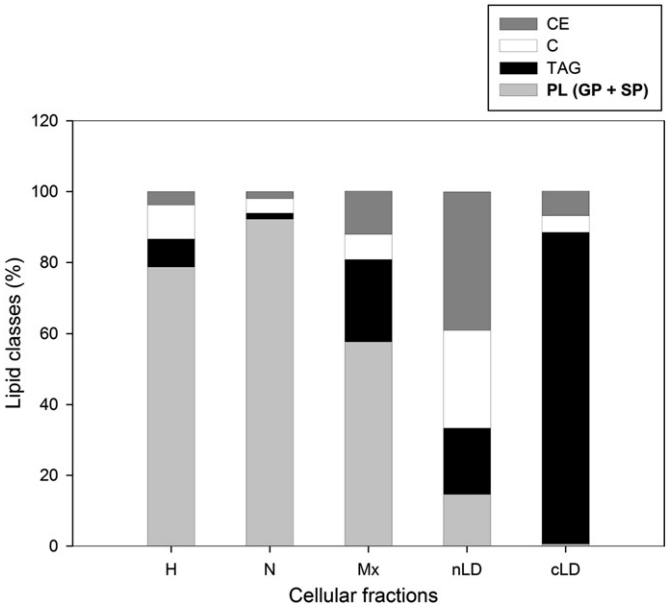

Fig. 10. Comparative lipid composition of rat-liver homogenates, nuclei, nuclear matrices, and nuclear- and cytosolic-lipid droplets. The data plotted were calculated from the results in Tables 1 and 2 that are expressed as nmol per g liver. Lipid classes are shown as a percent of the total: polar lipids (GP + SP) + neutral lipids (TAG, CE, and C). H, liver homogenate; N, nucleus; Mx, nuclear matrix; nLD, nuclear-lipid droplets; cLD, cytosolic-lipid droplets; PL, polar lipids; GP, glycerophospholipids; SP, sphingolipids; TAG, triacylglycerols; C, cholesterol; and CE, cholesteryl esters.

Since PI was found to be a component of the cLD monolayer [42], PI could also be present in nLD and would represent an endonuclear source of that phospholipid for the nuclear signal-transduction system that has been previously described [47]. Moreover, because the protein and lipid components of the nuclear-PI–signal-transduction system were seen to be either associated with or anchored to the Mx [48–50], those constituents could be located in the nLD monolayer.

Despite different subcellular localizations, the TAG from nLD and from cLD have similar FA compositions, with both being characterized by oleate and linoleate as the unsaturates and palmitate as the principal saturated FA. Moreover, TG (18:1/18:2/16:0) molecular species have been identified in cLD isolated from different cell lines [42].

Nuclear lipids play an active role in cell proliferation, differentiation, and apoptosis. nLD could thus be involved in nuclear-lipid homeostasis and serve as an endonuclear buffering system that can rapidly provide or incorporate lipids involved in these processes. The ultimate role of the nLD lipids could be the regulation of enzymes involved in nuclear-lipid metabolism, signaling events, and/or interactions with transcription factors such as the PPAR and the HNF 4 α that have FA as ligands [51]. Moreover, when these processes are shut down and the bound lipids (e.g., the FA, DG, phosphoinositides) are accordingly released from the specific active site and/or receptor, these lipidic regulatory ligands could become incorporated into nLD. We cannot discard the possibility that nLD could move within the nucleus and deliver lipids and proteins to different nuclear domains. In this regard, nuclear actin and myosin, in their function as cell-motility proteins, could possibly be involved in nLD transport within the nucleus [52].

We evaluated the size of the FA pool esterified to the different lipid classes assuming that GP, SP, TAG, and CE contained, 2, 1, 3, and 1 FA esterified per molecule, respectively. In the Mx, FA were esterified to both PL (58%) and NL (42%), Table 1. The FA pools esterified to TAG (36%) and PC (30%) were greater than the PE-associated pool (11%) (Table 1 and [3]). Moreover, the FA pool esterified to CE (6%) was comparable in size to those of PI (9%), PS (5%), and SM (3%). As expected, NL (TAG and CE) were the main FA pools in nLD. Thus, within the nucleus, TAG and PC were the lipid classes with the largest fatty-acyl pool.

Neutral lipids have been shown to be nuclear constituents in a number of species [6,7,53,54]. Since we found that nuclear NL are organized in droplets, we propose that nLD are present in most mammalian cells. Moreover, we would surmise that, as with rat liver, the nuclear NL in rat kidney likewise would be organized in nLD since arachidonic acid in isolated kidney nuclei was esterified not only to GP, as with liver, but also to TAG by an acyl-CoA-dependent mechanism [22].

Almost all cell types—including both prokaryotes and eukaryotes—have been reported to accumulate NL in cLD [55–58]. In eukaryotic cells, cLD were seen to be formed on the endoplasmic reticulum, and several mechanisms have been proposed to explain this process [58]. Because the nuclear membrane is structurally continuous with the endoplasmic reticulum, nLD could well be formed on the nuclear membrane.

At present, is difficult to determine the origin of nuclear CE stored in nLD, but two possibilities can be cited: 1) CE could be translocated from cytosol, where that class is in much greater abundance; 2) alternatively, could be synthesized in nucleus by esterification of nuclear C by an isoform different from ACAT-1 since Western blot failed to reveal that specific isoform in liver nuclei (Fig. 1). Accordingly, exogenous 20:4 ($n-6$) was found to become esterified to C of liver nuclei to form CE only when the FA had been previously activated as

arachidonyl-CoA [45]. Because of the low amount of nLD CE, we were unable to determine the FA composition, but previous analyses of the CE extracted from whole nuclei, had revealed that that fraction contained mainly esterified saturated (44%) and monoenoic (34%) FA along with low proportions of $n-6$ (17%) and $n-3$ (6%) polyunsaturates [38]. We now know that the nuclear CE characterized at that earlier time is mainly located in nLD.

In 1973 Shuichui Karasaki [59] observed "osmiophilic" nuclear zones by TEM in histological samples of liver nodules in preneoplastic rats after 3 to 4 months of a diet with the carcinogenic azo dye "butter yellow" [60]. He considered that such osmiophilic structures were LD, but no biochemical determinations or experimental evidence other than TEM images were presented. We cannot disregard the possibility that the osmiophilic zones observed in those preneoplastic liver nodules were the characteristic nuclear canaliculi structures of cancerous cells and tissues consisting of invaginations into the nucleus of either the inner nuclear membrane alone or the whole nuclear-membrane. In a transverse section of a histological sample by TEM such canaliculi structures are observed as round vesicles surrounded by one or two membranes [61,62].

Furthermore, under normal growth conditions most cell nuclei have a nucleoplasmic reticulum (NR) comprised of an intranuclear network of membranes that communicates with the cytosol or the intermembrane space [63]. The nLD must be a domain entirely different from nuclear-envelope invaginations since those droplets had proved resistant to the Triton X-100 utilized during the isolation of the nuclear-matrix and were thereafter visualized within that isolate. By contrast, nuclear-membrane invaginations would have been eliminated together with the rest of the nuclear membrane. Moreover, we consider that the nLD cannot be cLD trapped within a nuclear invagination since the cLD-marker protein PLIN 1 is absent and the cLD and nLD have markedly different lipid compositions.

5. Conclusions

nLD are a new class of subnuclear bodies and a nuclear domain where NL are stored and organized. These droplets would be built up around a hydrophobic core of TAG and CE enriched in oleic acid and surrounded by a monolayer of PL along with C and associated proteins. Thus, within nucleus, the lipids would have two main locations: the double- nuclear-membrane (composed mainly of GP, SP, and C) and nLD (containing principally TAG, CE, and C). Both of these domains would constitute alternative lipid sources with different chemical compositions, physical properties, functions, and regulatory characteristics.

Supplementary data to this article can be found online at http://dx.doi.org/10.1016/j.bbalip.2012.10.005.

Acknowledgements

This work was financially supported by the following grants: Universidad Nacional de La Plata (UNLP), Consejo Nacional de Investigaciones Científicas y Tecnológicas (CONICET) and Agencia de Promoción Científica y Tecnológica (ANPCyT) from Argentina. The authors are grateful to María Cristina Pallanza for the technical assistance and thank Prof. S. Demichelis, Statistical Advisor, for the statistical analysis.

References

[1] A. Ves-Losada, R.R. Brenner, Fatty acid delta 5 desaturation in rat liver cell nuclei, Mol. Cell. Biochem. 142 (1995) 163–170.
[2] S.M. Mate, J.P. Layerenza, A. Ves-Losada, Incorporation of arachidonic and stearic acids bound to L-FABP into nuclear and endonuclear lipids from rat liver cells, Lipids 42 (2007) 589–602.
[3] S.M. Mate, R.R. Brenner, A. Ves-Losada, Endonuclear lipids in liver cells, Can. J. Physiol. Pharmacol. 84 (2006) 459–468.
[4] E. Albi, M. Mersel, C. Leray, M.L. Tomassoni, M.P. Viola-Magni, Rat liver chromatin phospholipids, Lipids 29 (1994) 715–719.
[5] A.N. Hunt, G.T. Clark, G.S. Attard, A.D. Postle, Highly saturated endonuclear phosphatidylcholine is synthesized in situ and colocated with CDP-choline pathway enzymes, J. Biol. Chem. 276 (2001) 8492–8499.
[6] H. Kleinig, Nuclear membranes from mammalian liver. II. Lipid composition, J. Cell Biol. 46 (1970) 396–402.
[7] T.W. Keenan, R. Berezney, L.K. Funk, F.L. Crane, Lipid composition of nuclear membranes isolated from bovine liver, Biochim. Biophys. Acta 203 (1970) 547–554.
[8] H. Fukuda, H. Tatsumi, N. Iritani, A. Katsurada, C. Kinoshita, H. Fujita, T. Tanaka, Lipogenic enzyme induction and incorporation of exogenous fatty acid into liver and liver nuclei, Biochim. Biophys. Acta 960 (1988) 19–25.
[9] E. Albi, I. Peloso, M.V. Magni, Nuclear membrane sphingomyelin-cholesterol changes in rat liver after hepatectomy, Biochem. Biophys. Res. Commun. 262 (1999) 692–695.
[10] G. Blobel, V.R. Potter, Nuclei from rat liver: isolation method that combines purity with high yield, Science 154 (1966) 1662–1665.
[11] C.B. Kasper, Isolation and properties of the nuclear envelope, Methods Enzymol. 31 (1974) 279–292.
[12] S.M. Actis Dato, A. Catala, R.R. Brenner, Circadian rhythm of fatty acid desaturation in mouse liver, Lipids 8 (1973) 1–6.
[13] L.R. Vann, F.B. Wooding, R.F. Irvine, N. Divecha, Metabolism and possible compartmentalization of inositol lipids in isolated rat-liver nuclei, Biochem. J. 327 (Pt. 2) (1997) 569–576.
[14] O.H. Lowry, N.J. Rosebrough, A.L. Farr, R.J. Randall, Protein measurement with the Folin phenol reagent, J. Biol. Chem. 193 (1951) 265–275.
[15] L. Kuerschner, C. Moessinger, C. Thiele, Imaging of lipid biosynthesis: how a neutral lipid enters lipid droplets, Traffic 9 (2008) 338–352.
[16] M.V. Yusenko, T. Ruppert, G. Kovacs, Analysis of differentially expressed mitochondrial proteins in chromophobe renal cell carcinomas and renal oncocytomas by 2-D gel electrophoresis, Int. J. Biol. Sci. 6 (2010) 213–224.
[17] I. Sabolic, C.M. Herak-Kramberger, S. Breton, D. Brown, Na/K-ATPase in intercalated cells along the rat nephron revealed by antigen retrieval, J. Am. Soc. Nephrol. 10 (1999) 913–922.
[18] X. Tao, Y. Jihong, G. Li, F. Bin, Z. Yi, C. Xiaodong, Z. Peichao, Z. Yang, Cloning, chromosome mapping and expression pattern of porcine PLIN and M6PRBP1 genes, Genet. Sel. Evol. 40 (2008) 215–226.
[19] J.P. Humbert, N. Matter, J.C. Artault, P. Koppler, A.N. Malviya, Inositol 1,4,5-trisphosphate receptor is located to the inner nuclear membrane indicating regulation of nuclear calcium signaling by inositol 1,4,5-trisphosphate. Discrete distribution of inositol phosphate receptors to inner and outer nuclear membranes, J. Biol. Chem. 271 (1996) 478–485.
[20] K. Furukawa, N. Pante, U. Aebi, L. Gerace, Cloning of a cDNA for lamina-associated polypeptide 2 (LAP2) and identification of regions that specify targeting to the nuclear envelope, EMBO J. 14 (1995) 1626–1636.
[21] J. Folch, M. Lees, G.H. Sloane Stanley, A simple method for the isolation and purification of total lipides from animal tissues, J. Biol. Chem. 226 (1957) 497–509.
[22] S.M. Mate, J.P. Layerenza, A. Ves-Losada, Arachidonic acid pools of rat kidney cell nuclei, Mol. Cell. Biochem. 345 (2010) 259–270.
[23] A. Ves-Losada, R.O. Peluffo, Effect of cold environment on hepatic microsomal delta 6 and delta 9 desaturase activity of male rats, Lipids 22 (1987) 583–588.
[24] W.W. Christie, X. Han, Lipid Analysis: Isolation, Separation, Identification and Lipidomic Analysis, Oily Press, The Bridgwater, 2010.
[25] W.R. Morrison, L.M. Smith, Preparation of fatty acid methyl esters and dimethylacetals from lipids with boron fluoride–methanol, J. Lipid Res. 5 (1964) 600–608.
[26] M.P. Polo, R. Crespo, M.G. de Bravo, Geraniol and simvastatin show a synergistic effect on a human hepatocarcinoma cell line, Cell Biochem. Funct. 29 (2011) 452–458.
[27] J.A. Ontko, L.W. Perrin, L.S. Horne, Isolation of hepatocellular lipid droplets: the separation of distinct subpopulations, J. Lipid Res. 27 (1986) 1097–1103.
[28] M.M. Bradford, A rapid and sensitive method for the quantitation of microgram quantities of protein utilizing the principle of protein-dye binding, Anal. Biochem. 72 (1976) 248–254.
[29] S. Siegel, N.J. Castellan, Nonparametric Statistics for the Behavioral Sciences, McGraw-Hill, 1988.
[30] R. Sikstrom, J. Lanoix, J.J. Bergeron, An enzymic analysis of a nuclear envelope fraction, Biochim. Biophys. Acta 448 (1976) 88–102.
[31] W.W. Franke, U. Scheer, G. Krohne, E.D. Jarasch, The nuclear envelope and the architecture of the nuclear periphery, J. Cell Biol. 91 (1981) 39s–50s.
[32] W.J. Arion, L.O. Schulz, A.J. Lange, J.N. Telford, H.E. Walls, The characteristics of liver glucose-6-phosphatase in the envelope of isolated nuclei and microsomes are identical, J. Biol. Chem. 258 (1983) 12661–12669.
[33] D.J. Murphy, The dynamic roles of intracellular lipid droplets: from archaea to mammals, Protoplasma (2011), http://dx.doi.org/10.1007/s00709-011-0329-7.
[34] T. Fujimoto, Y. Ohsaki, J. Cheng, M. Suzuki, Y. Shinohara, Lipid droplets: a classic organelle with new outfits, Histochem. Cell Biol. 130 (2008) 263–279.
[35] D.L. Spector, A.I. Lamond, Nuclear speckles, Cold Spring Harb. Perspect. Biol. 3 (2011) a000646.
[36] A.H. Fox, A.I. Lamond, Paraspeckles, Cold Spring Harb. Perspect. Biol. 2 (2010) a000687.
[37] D. DiDonato, D.L. Brasaemle, Fixation methods for the study of lipid droplets by immunofluorescence microscopy, J. Histochem. Cytochem. 51 (2003) 773–780.
[38] S.M. Mate, R.R. Brenner, A. Ves-Losada, Phosphatidyl choline fatty acid remodeling in the hepatic cell nuclei, Prostaglandins Leukot. Essent. Fatty Acids 70 (2004) 49–57.

[39] D.J. Murphy, The biogenesis and functions of lipid bodies in animals, plants and microorganisms, Prog. Lipid Res. 40 (2001) 325–438.
[40] N.O. Favale, M.C. Fernandez-Tome, L.G. Pescio, N.B. Sterin-Speziale, The rate-limiting enzyme in phosphatidylcholine synthesis is associated with nuclear speckles under stress conditions, Biochim. Biophys. Acta 1801 (2010) 1184–1194.
[41] E. Albi, M.P. Viola Magni, The role of intranuclear lipids, Biol. Cell 96 (2004) 657–667.
[42] R. Bartz, W.H. Li, B. Venables, J.K. Zehmer, M.R. Roth, R. Welti, R.G. Anderson, P. Liu, K.D. Chapman, Lipidomics reveals that adiposomes store ether lipids and mediate phospholipid traffic, J. Lipid Res. 48 (2007) 837–847.
[43] G.w.M. Villani, M. Tosti, F. Marini, E. Bartoccini, M.V. Magni, E. Albi, Lipid microdomains in cell nucleus, Mol. Biol. Cell 19 (2008) 5289–5295.
[44] A. Ves-Losada, R.R. Brenner, Long-chain fatty Acyl-CoA synthetase enzymatic activity in rat liver cell nuclei, Mol. Cell. Biochem. 159 (1996) 1–6.
[45] A. Ves-Losada, S.M. Mate, R.R. Brenner, Incorporation and distribution of saturated and unsaturated fatty acids into nuclear lipids of hepatic cells, Lipids 36 (2001) 273–282.
[46] A. Ves-Losada, R.R. Brenner, Incorporation of delta 5 desaturase substrate (dihomogammalinolenic acid, 20:3 n-6) and product (arachidonic acid 20:4 n-6) into rat liver cell nuclei, Prostaglandins Leukot. Essent. Fatty Acids 59 (1998) 39–47.
[47] N.M. Maraldi, N. Zini, S. Santi, F.A. Manzoli, Topology of inositol lipid signal transduction in the nucleus, J. Cell. Physiol. 181 (1999) 203–217.
[48] R.F. Irvine, Nuclear lipid signalling, Nat. Rev. Mol. Cell Biol. 4 (2003) 349–360.
[49] C.S. D'Santos, J.H. Clarke, N. Divecha, Phospholipid signalling in the nucleus. Een DAG uit het leven van de inositide signalering in de nucleus, Biochim. Biophys. Acta 1436 (1998) 201–232.
[50] B. Payrastre, M. Nievers, J. Boonstra, M. Breton, A.J. Verkleij, P.M. Bergen en Henegouwen, A differential location of phosphoinositide kinases, diacylglycerol kinase, and phospholipase C in the nuclear matrix, J. Biol. Chem. 267 (1992) 5078–5084.
[51] M. Elholm, A. Garras, S. Neve, D. Tornehave, T.B. Lund, J. Skorve, T. Flatmark, K. Kristiansen, R.K. Berge, Long-chain acyl-CoA esters and acyl-CoA binding protein are present in the nucleus of rat liver cells, J. Lipid Res. 41 (2000) 538–545.
[52] E. Castano, V. Philimonenko, M. Kahle, J. Fukalová, A. Kalendová, S. Yildirim, R. Dzijak, H. Dingová-Krásna, P. Hozák, Actin complexes in the cell nucleus: new stones in an old field, Histochem. Cell Biol. 133 (2010) 607–626.
[53] E. Albi, S. Cataldi, G. Rossi, M.V. Magni, A possible role of cholesterol–sphingomyelin/phosphatidylcholine in nuclear matrix during rat liver regeneration, J. Hepatol. 38 (2003) 623–628.
[54] J.R. Tata, Isolation of nuclei from liver and other tissues, Methods Enzymol. 31 (1974) 253–262.
[55] R.A. Silva, V. Grossi, N.L. Olivera, H.M. Alvarez, Characterization of indigenous *Rhodococcus* sp. 602, a strain able to accumulate triacylglycerides from naphthyl compounds under nitrogen-starved conditions, Res. Microbiol. 161 (2010) 198–207.
[56] M. Digel, R. Ehehalt, J. Fullekrug, Lipid droplets lighting up: insights from live microscopy, FEBS Lett. 584 (2010) 2168–2175.
[57] H. Mu, C.E. Hoy, The digestion of dietary triacylglycerols, Prog. Lipid Res. 43 (2004) 105–133.
[58] T.C. Walther, R.V. Farese Jr., The life of lipid droplets, Biochim. Biophys. Acta 1791 (2009) 459–466.
[59] S. Karasaki, Passage of cytoplasmic lipid into interphase nuclei in preneoplastic rat liver, J. Ultrastruct. Res. 42 (1973) 463–478.
[60] E.L. Opie, The pathogenesis of tumors of the liver produced by butter yellow, J. Exp. Med. 80 (1944) 231–246.
[61] S. Karasaki, An electron microscope study of intranuclear canaliculi in Novikoff hepatoma cells, Cancer Res. 30 (1970) 1736–1742.
[62] O. Kawanami, V.J. Ferrans, J.D. Fulmer, R.G. Crystal, Nuclear inclusions in alveolar epithelium of patients with fibrotic lung disorders, Am. J. Pathol. 94 (1979) 301–322.
[63] A. Malhas, C. Goulbourne, D.J. Vaux, The nucleoplasmic reticulum: form and function, Trends Cell Biol. 21 (2011) 362–373.